JCB Article

PKA phosphorylation activates the calcium release channel (ryanodine receptor) in skeletal muscle: defective regulation in heart failure

Steven Reiken,[1] Alain Lacampagne,[5] Hua Zhou,[4] Aftab Kherani,[4] Stephan E. Lehnart,[1] Chris Ward,[5] Fannie Huang,[1] Marta Gaburjakova,[1] Jana Gaburjakova,[1] Nora Rosemblit,[1] Michelle S. Warren,[4] Kun-lun He,[2] Geng-hua Yi,[2] Jie Wang,[2] Daniel Burkhoff,[2] Guy Vassort,[5] and Andrew R. Marks[1,3]

[1]Center for Molecular Cardiology, [2]Circulatory Physiology Division, Department of Medicine, [3]Department of Pharmacology, and [4]Cardiothoracic Surgery Division, Columbia University College of Physicians and Surgeons, New York, NY 10032
[5]Physiopathologie Cardiovasculaire, INSERM U390, Montpellier, France

The type 1 ryanodine receptor (RyR1) on the sarcoplasmic reticulum (SR) is the major calcium (Ca^{2+}) release channel required for skeletal muscle excitation–contraction (EC) coupling. RyR1 function is modulated by proteins that bind to its large cytoplasmic scaffold domain, including the FK506 binding protein (FKBP12) and PKA. PKA is activated during sympathetic nervous system (SNS) stimulation. We show that PKA phosphorylation of RyR1 at Ser^{2843} activates the channel by releasing FKBP12. When FKB12 is bound to RyR1, it inhibits the channel by stabilizing its closed state. RyR1 in skeletal muscle from animals with heart failure (HF), a chronic hyperadrenergic state, were PKA hyperphosphorylated, depleted of FKBP12, and exhibited increased activity, suggesting that the channels are "leaky." RyR1 PKA hyperphosphorylation correlated with impaired SR Ca^{2+} release and early fatigue in HF skeletal muscle. These findings identify a novel mechanism that regulates RyR1 function via PKA phosphorylation in response to SNS stimulation. PKA hyperphosphorylation of RyR1 may contribute to impaired skeletal muscle function in HF, suggesting that a generalized EC coupling myopathy may play a role in HF.

Introduction

Ryanodine receptors (RyRs)* are calcium (Ca^{2+}) release channels on the sarcoplasmic reticulum (SR) of striated muscles that are required for excitation–contraction (EC) coupling. In skeletal muscle, the type 1 RyR (RyR1) is a tetramer comprised of four 565,000-D RyR1 polypeptides and four 12,000-D FK-506 binding proteins (FKBP12). FKBP12s are regulatory subunits that stabilize RyR channel function (Brillantes et al., 1994) and facilitate coupled gating between neighboring RyR channels (Marx et al., 1998) that are packed into dense arrays in specialized regions of the SR that release intracellular stores of Ca^{2+}, which triggers muscle contraction.

In addition to FKBP12, the RyR1 macromolecular complex includes the catalytic and regulatory subunits of PKA and protein phosphatase 1 (PP1) (Marx et al., 2001). In skeletal muscle, EC coupling is triggered by charge movement in the voltage-gated Ca^{2+} channel (VGCC) in the transverse tubule that leads to activation of RyR1, presumably via a direct interaction between the VGCC and RyR1 (Schneider and Chandler, 1973; Rios and Brum, 1987). This mechanism is distinct from that in the heart where the cardiac RyR2 is activated by Ca^{2+} influx through the VGCC, a process known as Ca^{2+}-induced Ca^{2+} release (Fabiato, 1983; Nabauer et al., 1989). However, Ca^{2+}-induced Ca^{2+} release may also play a role in regulating RyR1 in skeletal-type EC coupling (Stern et al., 1997).

One FKBP12 molecule is bound to each RyR1 subunit, and dissociation of FKBP12 increases the open probability (P_o) of the channel (Brillantes et al., 1994; Gaburjakova et

Address correspondence to Andrew R. Marks, Center for Molecular Cardiology, Box 65, Columbia University College of Physicians and Surgeons, Room 9-401, 630 West 168th Street, New York, NY 10032. Tel.: (212) 305-0270. Fax: (212) 305-3690. E-mail: arm42@columbia.edu

C. Ward's present address is University of Maryland School of Nursing, Baltimore, MD.

*Abbreviations used in this paper: EC, excitation–contraction; HF, heart failure; LV, left ventricular, mAKAP, muscle A-kinase anchoring protein; P_o, open probability; PP1, protein phosphatase 1; RyR, ryanodine receptor; RyR1, type 1 RyR; SNS, sympathetic nervous system; SR, sarcoplasmic reticulum; VGCC, voltage-gated Ca^{2+} channel; WT, wild type.

Key words: ryanodine receptor; heart failure; skeletal muscle; excitation–contraction coupling; FKBP12

al., 2001). In addition, dissociation of FKBP12 from RyR1 channels inhibits coupled gating, resulting in channels that gate stochastically rather than as an ensemble (Marx et al., 1998). FKBPs are cis–trans peptidyl–prolyl isomerases that are widely expressed and subserve a variety of cellular functions (Marks, 1996). FKBP12s are tightly bound to and regulate the function of the skeletal (RyR1) (Jayaraman et al., 1992; Brillantes et al., 1994) and cardiac (RyR2) (Kaftan et al., 1996) muscle Ca^{2+} release channels.

RyR1 and RyR2 channels in skeletal and cardiac muscles, respectively, are substrates for phosphorylation by PKA, which activates the channel via an unknown mechanism (Seiler et al., 1984; Takasago et al., 1989; Suko et al., 1993; Hain et al., 1995; Valdivia et al., 1995; Marx et al., 2000, 2001; Uehara et al., 2002). PKA is targeted to both skeletal RyR1 and cardiac RyR2 (Marx et al., 2000, 2001). To gain a better understanding of the mechanism by which PKA phosphorylation regulates the function of RyR1, we used alanine substitution to identify the unique PKA phosphorylation site on RyR1 (Ser^{2843}) and generated mutant channels that either mimic constitutively PKA-phosphorylated RyR1 or cannot be PKA phosphorylated. Constitutively PKA-phosphorylated RyR1 was unable to bind FKBP12 and exhibited single channel properties similar to those of RyR1 containing mutations in the FKBP12 binding site that also does not bind FKBP12. To examine the physiologic role of PKA phosphorylation, we studied channels isolated from skeletal muscle from animal models of heart failure (HF), which is a hyperadrenergic state.

RyR1 from canine and rat models of HF was PKA hyperphosphorylated and depleted of FKBP12. These biochemical changes caused increased activity (P_o) and increased gating kinetics of the RyR1 from HF skeletal muscle. These findings suggest that FKBP12 stabilizes the open and closed states of RyR1 and that PKA phosphorylation regulates RyR1 function, in part, via dissociation of FKBP12. Consistent with the depletion of FKBP12 from the RyR1 channels from HF skeletal muscle, which inhibits RyR1 coupled gating (Marx et al., 1998), the rate of SR Ca^{2+} release and the decay of the Ca^{2+} transient were both slowed in HF skeletal muscle (measured as spontaneous Ca^{2+} release events or Ca^{2+} sparks). These defects in RyR1 and SR Ca^{2+} release were associated with early fatigue in HF skeletal muscle. Many patients with moderate degrees of cardiac dysfunction have substantially reduced exercise capacity that cannot be explained solely by the extent of their HF (Minotti et al., 1991; Sullivan and Hawthorne, 1995). This has led to the hypothesis that a primary skeletal muscle defect exists in patients with HF in addition to a primary cardiac muscle defect.

Results

PKA phosphorylation of Ser^{2843} in RyR1 regulates FKBP12 binding and activates the channel

We identified the PKA phosphorylation site on RyR1 using site-directed mutagenesis and examined the effects of PKA phosphorylation of this site on the composition and function of the RyR1 macromolecular signaling complex (Marx et al., 2001). Alanine (RyR1-S2843A) and aspartic acid (RyR1-S2843D) substitutions were used to identify

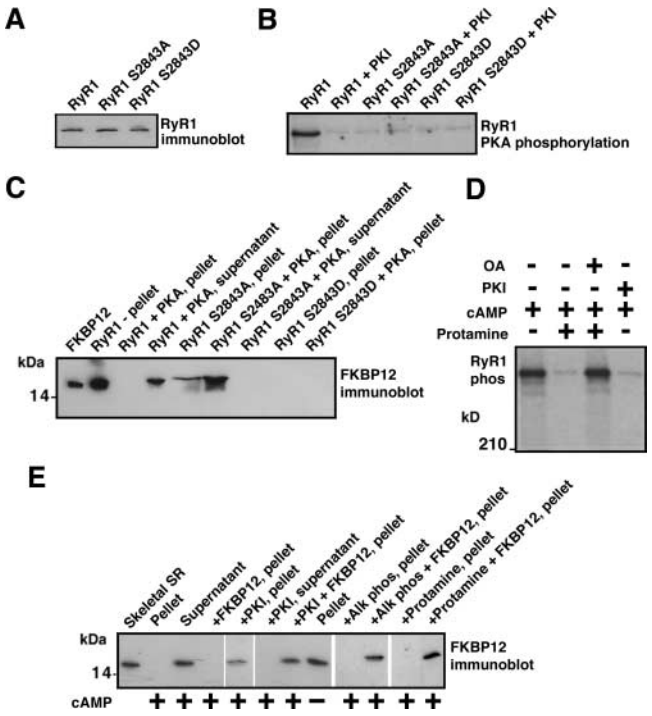

Figure 1. **FKBP12 binding to RyR1 is regulated by PKA phosphorylation of RyR1-Ser^{2843}.** (A) Immunoblot showing that equivalent amounts of WT and mutant (RyR1-S2843A and RyR1-S2843D) RyR1 were expressed in HEK293 cells. (B) Autoradiograph showing PKA phosphorylation of RyR1 using γP^{32}-ATP (PKI_{5-24} was used to show specificity of the kinasing reaction). Alanine substitution identified Ser^{2843} as the unique PKA phosphorylation site on RyR1. (C) Immunoblot showing binding of FKBP12 to WT and mutant RyR1, assessed by centrifugation (FKBP12 cosediments with RyR1) and FKBP12 immunoblotting. FKBP12 does not bind to RyR1-S2843D, which mimics constitutively PKA-phosphorylated RyR1. (D) Autoradiograph showing that activation of PKA bound to RyR1 with cAMP causes phosphorylation of the channel, which is inhibited by the PKA inhibitor PKI_{5-24}. Activation of PP1 bound to the channel with protamine causes dephosphorylation of the channel, which is blocked by okadaic acid (OA). (E) FKBP12 immunoblot showing that cAMP-induced PKA phosphorylation of RyR1 dissociates FKBP12 from the channel complex. FKBP12 cannot bind to the PKA-phosphorylated channel, but dephosphorylation of the channel with alkaline phosphatase (or by activating bound phosphatases with protamine) allows subsequent rebinding of FKBP12 to the channel, as assessed by cocentrifugation.

Ser^{2843} as the unique PKA phosphorylation site on RyR1 (Fig. 1, A and B). RyR1-S2843A and RyR1-S2843D were expressed in HEK293 cells with same efficiency as the wild-type (WT) RyR1 (Fig. 1 A). FKBP12 binding to RyR1 was assessed by coprecipitation (Fig. 1 C) as previously described (Gaburjakova et al., 2001). FKBP12 was detected by immunoblot in the pellet only when bound to RyR1, otherwise, FKBP12 was detected in the supernatant. PKA phosphorylation of RyR1 at Ser^{2843} (homologous to the PKA phosphorylation site on RyR2, Ser^{2809}; Marx et al., 2000) resulted in the dissociation of FKBP12 from WT RyR1, but not from mutant RyR1-S2843A, which could not be PKA phosphorylated (Fig. 1 C). FKBP12 bound to the mutant RyR1-S2483A but not to the mutant RyR1-S2483D, which mimics the constitutively PKA-phosphorylated RyR1. These data establish

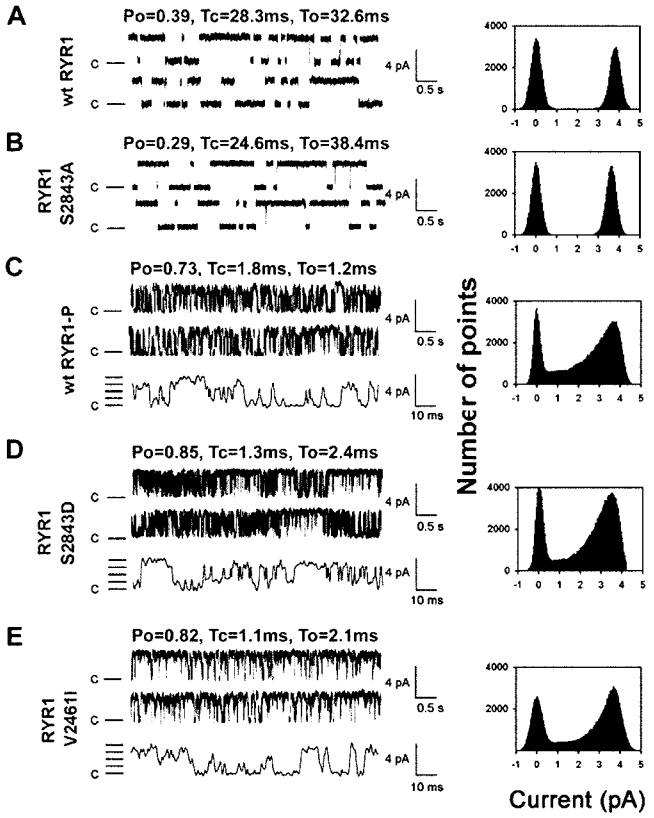

Figure 2. **PKA phosphorylation of Ser^{2843} activates RyR1 channels.** (A) Representative single channel tracings of WT RyR1, (B) RyR1-S2843A, (C) PKA-phosphorylated WT RyR1, (D) RyR1-S2843D, and (E) RyR1-V2461I (this mutant RyR1 was previously shown to bind FKBP12.6 but not FKBP12; Gaburjakova et al., 2001). RyR1 single channel recordings in planar lipid bilayers show activity of the channels at 150 nM $[Ca^{2+}]_{cis}$ with 1 mM ATP. Recordings were at 0 mV, closed state of the channels are indicated as C, and openings are upwards. All point amplitude histograms are shown. P_o and mean closed (Tc) and open (To) dwell times are shown above each channel tracing.

that PKA phosphorylation of RyR1 at Ser^{2843} regulates binding of FKBP12 to the RyR1 channel.

We previously showed that PKA and PP1 are targeted to RyR1 via targeting proteins that bind to highly conserved leucine/isoleucine zipper motifs on the channel (Marx et al., 2001). PKA bound to RyR1 was activated with cAMP (10 μM), causing PKA phosphorylation of RyR1 (Fig. 1 D). PP1 bound to RyR1 was activated with protamine (1 mg/ml), causing dephosphorylation of RyR1 (Fig. 1 D). Thus, PKA and PP1 in the RyR1 macromolecular complex can regulate phosphorylation/dephosphorylation of the channel without addition of exogenous kinase or phosphatase.

The effects of activation of PKA in the RyR1 macromolecular complex on FKBP12 binding to RyR1 were assessed by coprecipitation (Fig. 1 E) as previously described (Gaburjakova et al., 2001). cAMP-induced PKA phosphorylation of RyR1 caused FKBP12 dissociation from RyR1 (Fig. 1 E). Excess FKBP12 could not bind to the PKA-phosphorylated RyR1. Inhibiting cAMP-induced activation of bound PKA with $PKI_{5–24}$ (500 nM) blocked phosphorylation-induced dissociation of FKBP12 from RyR1 (Fig. 1 E). After PKA-phosphorylated RyR1 was dephosphorylated with alkaline phosphatase (1 U/mg of SR protein) or by activating bound phosphatase (PP1) with protamine (1 mg/ml), FKBP12 could rebind to the channel (Fig. 1 E). Thus, PKA phosphorylation dissociates FKBP12 from RyR1, and FKBP12 cannot rebind to PKA-phosphorylated RyR1.

To determine the functional affects of PKA phosphorylation of RyR1, we expressed RyR1 in HEK293 cells and reconstituted recombinant channels in planar lipid bilayers to examine their single channel properties (Fig. 2 A). WT RyR1 channels (Fig. 2 A) were compared to (a) mutant channels that cannot be PKA phosphorylated (RyR1-S2843A; Fig. 2 B), (b) PKA-phosphorylated WT RyR1 (Fig. 2 C), (c) mutant RyR1 that mimics constitutively PKA-phosphorylated RyR1 (RyR1-S2843D; Fig. 2 D), and (d) mutant RyR1 that cannot bind FKBP12 (RyR1-S2461I; Fig. 2 E). WT RyR1 exhibited the same single channel properties as native RyR1 (Fig. 2 A; Table I), as previously reported (Brillantes et al., 1994; Gaburjakova et al., 2001). Mutant RyR1-S2843A also exhibited the same single channel properties as native RyR1 (Fig. 2 B).

PKA phosphorylation of RyR1 activated WT RyR1 (increased P_o and decreased open and closed dwell times; Fig. 2 C; Table I). PKA phosphorylation of WT RyR1 was confirmed by back phosphorylation (Fig. 1 B). RyR1-S2843A cannot be activated by PKA, indicating that activation of WT RyR1 by PKA was due to PKA phosphorylation of RyR1, because the only difference between the WT and mutant RyR1-S843A channels is that the latter cannot be phosphorylated by PKA due to a Ser^{2843}Ala substitution. RyR1-S2843D exhibited the same single channel properties as PKA-phosphorylated WT RyR1 (Fig. 2 D; Table I), providing additional evidence that the affects of PKA phosphorylation on RyR1 are due to phosphorylation of Ser^{2843}. Thus, PKA phosphorylation of RyR1 potently activates the channel at 150 nM cis (cytoplasmic) $[Ca^{2+}]_{cis}$. Because PKA phosphorylation of RyR1 causes dissociation of FKBP12

Table I. **PKA phosphorylation activates RyR1**

	Nonphosphorylated			PKA phosphorylated		
	Open probability	Open time	Closed time	Open probability	Open time	Closed time
		ms	*ms*		*ms*	*ms*
RyR1 (n = 21)	0.34 ± 0.1[a]	22.1 ± 2.4[a]	36.7 ± 3.4[a]	0.72 ± 0.1[a]	1.6 ± 0.6[a]	1.4 ± 0.5[a]
RyR1-S2843A (n = 11)	0.29 ± 0.1	25.1 ± 2.1	34.4 ± 2.4	ND	ND	ND
RyR1-S2843D (n = 14)	0.81 ± 0.3[b]	1.1 ± 0.3[b]	1.9 ± 0.8[b]	ND	ND	ND

[a]$P < 0.001$ for nonphosphorylated versus PKA phosphorylated.
[b]$P < 0.001$ for RyR1-S2843D versus nonphosphorylated WT.

from the channel (Fig. 1 C), we sought to determine whether the activation of RyR1 by PKA phosphorylation is due to dissociation of FKBP12 from the channel. To address this question, we compared the single channel properties of RyR1-V2461I, which cannot bind FKBP12 due to a mutation in the FKBP12 binding site (Gaburjakova et al., 2001), with those of PKA-phosphorylated RyR1. RyR1-V2461I exhibited the same changes in single channel properties as PKA-phosphorylated WT RyR1 and the RyR1-S2843D mutant channel; increased P_o and decreased open and closed dwell times compared with nonphosphorylated WT channels (Fig. 2 E; Table I).

FKBP12.6 is homologous to FKBP12 and is able to bind to RyR1-V2461I, whereas FKBP12 cannot (Gaburjakova et al., 2001). We showed previously that the altered single channel properties of the RyR1-V2461I channels, increased P_o and decreased open and closed dwell times, can be restored to normal by FKBP12.6 binding to the channel (Gaburjakova et al., 2001). Thus, the increased P_o and decreased open and closed dwell times exhibited by the RyR1-V2461I mutant channels are specifically due to lack of binding of FKBP12, rather than some undefined effect of the mutation on channel structure or function. Taken together, these data indicate that the activation of RyR1 by PKA phosphorylation at Ser^{2843} is specifically due to dissociation of FKBP12 from the channel.

RyR1 PKA hyperphosphorylation and defective function in HF skeletal muscle

We sought to determine whether RyR1 channels from skeletal muscle from animal models of HF (a chronic hyperadrenergic condition) were PKA hyperphosphorylated and exhibited altered single channel properties. PKA phosphorylation of RyR1 from hind-limb skeletal muscle from a canine model of pacing-induced HF was assessed using immunoprecipitation of RyR1 followed by back phosphorylation (Fig. 3 A), as described previously (Marx et al., 2000). Hemodynamics showed that left ventricular (LV) dP/dt_{max} was 3420 ± 105 in controls and 1722.2 ± 322 in HF (mmHg/s; $n = 4$ normal, $n = 5$ HF; $P < 0.01$). RyR1 from HF skeletal muscle was PKA hyperphosphorylated compared with RyR1 from normal skeletal muscle (Fig. 3 A): normal 0.4 ± 0.2, HF 3.6 ± 0.8 moles phosphate transferred per mole of RyR1 channel ($n = 4$ normal, $n = 5$ HF; $P < 0.01$). Thus, 3/4–4/4 PKA sites on each RyR1 channel were phosphorylated in HF skeletal muscle, versus <1/4 sites in RyR1 from normal control skeletal muscle.

We previously showed that PKA hyperphosphorylation of cardiac RyR2 causes depletion of FKBP12.6 from the channel macromolecular complex, resulting in channels with altered gating properties in failing hearts (Marx et al., 2000). Using coimmunoprecipitations (Marx et al., 2000), we found that there was a significant reduction (approximately threefold) in the amount of FKBP12 in the RyR1 complex from HF skeletal muscle compared with controls ($n = 2$ control, $n = 5$ HF; $P < 0.01$; Fig. 3 B); comparable to the degree of depletion of FKBP12 from the RyR1 complex observed when RyR1 channels from normal skeletal muscle were subjected to in vitro PKA phosphorylation (Fig. 3 B).

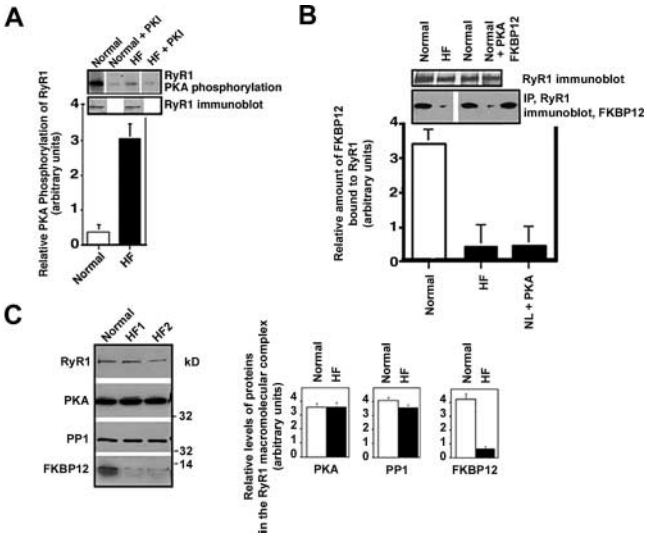

Figure 3. **RyR1 PKA hyperphosphorylation in HF skeletal muscle.** (A) PKA phosphorylation of RyR1 was measured in skeletal muscle homogenates from control normal dogs and dogs with pacing-induced HF. Equivalent amounts of RyR1 protein were used in each kinasing reaction, as shown by immunoblotting. The relative PKA phosphorylation of RyR1 from skeletal muscle homogenates from normals ($n = 2$) and HF animals ($n = 5$) was determined by dividing the specific phosphorylation signal by the amount of RyR1 protein (determined by immunoblotting and densitometry). Results are expressed as the inverse of the PKA-dependent [γ-^{32}P]ATP signal ± the SD of the mean. (B) The amount of FKBP12 bound to RyR1 was assessed by coimmunoprecipitation followed by immunoblotting. (C) Representative immunoblots are shown for components of the RyR1 macromolecular complex: RyR1, PKA, PP1, and FKBP12 using samples from normal ($n = 2$) and HF animals ($n = 5$). Protein levels were quantified using densitometry of immunoblots. Results are expressed as the relative amount of each of the components of the RyR1 macromolecular complex corrected for the amount of RyR1 in each immunoprecipitation. Error bars are SD of the mean.

The total amount of cellular FKBP12 (see Fig. 6 C), as well as the levels of the catalytic subunit of PKA, and the phosphatase PP1 in the RyR1 macromolecular complex were not changed (Fig. 3 C). Thus, PKA hyperphosphorylation of RyR1 is associated with depletion of FKBP12 from the RyR1 complex in HF skeletal muscle, analogous to the PKA hyperphosphorylation–induced depletion of FKBP12.6 from RyR2 in failing hearts (Marx et al., 2000).

HF RyR1 channels had increased P_o at cis (cytosolic) [Ca^{2+}] of 100 nM (Fig. 4, A and B; Table II). Normal RyR1 channels are not active at 100 nM $[Ca^{2+}]_{cis}$ (Meissner, 1994). HF RyR1 channels exhibited subconductance states or partial openings (Brillantes et al., 1994) that are rarely observed in RyR1 channels from normal skeletal muscle (Fig. 4 B; Table II). Coupled gating between RyR1 channels, a mechanism by which clusters of channels open and close simultaneously (Marx et al., 1998), was markedly reduced in HF skeletal muscle channels compared with RyR1 channels from controls (Table II). The mean open and closed dwell times were significantly reduced in HF RyR1 compared with control (Fig. 4, A and B; Table II). Increased P_o at submicromolar $[Ca^{2+}]_{cis}$, decreased open and closed dwell times, subconductance openings, and reduced coupled gating are features of recombinant RyR1 expressed without

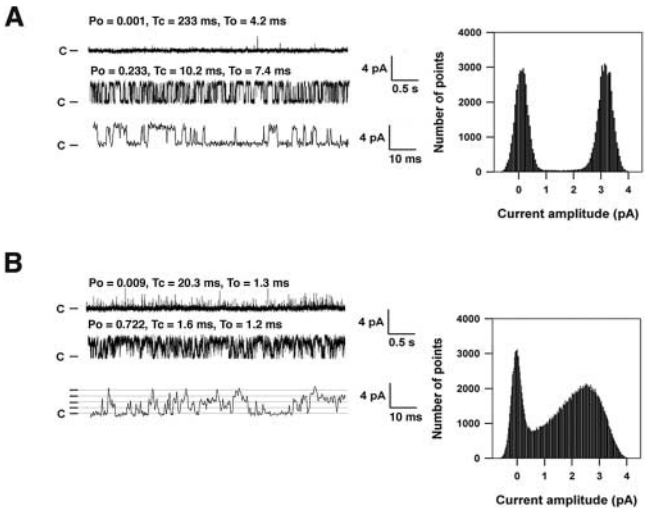

Figure 4. **Defective single channel properties of RyR1 isolated from skeletal muscle during HF.** (A) Single channel traces from an RyR1 channel from normal canine skeletal muscle and corresponding current amplitude histogram. (B) Single channel traces from an RyR1 channel from HF canine skeletal muscle and corresponding current amplitude histogram. In A and B, upper tracings were recorded at 100 nM $[Ca^{2+}]_{cis}$, and bottom tracings were recorded after activation of the RyR1 channels with 1 mM ATP to increase P_o. Open (T_o) and closed (T_c) dwell times and P_o are shown for each condition above the representative tracings. In A and B, the bottom tracing is an expanded time scale. Lines indicating the current levels (0, 1, 2, 3, 4 pA) for the subconductance states of the PKA-hyperphosphorylated channel are shown in the bottom tracing in B. All point amplitude histograms for each channel are shown. Recordings were at 0 mV, the closed state of the channels is indicated as C, and the channel openings are upward deflections.

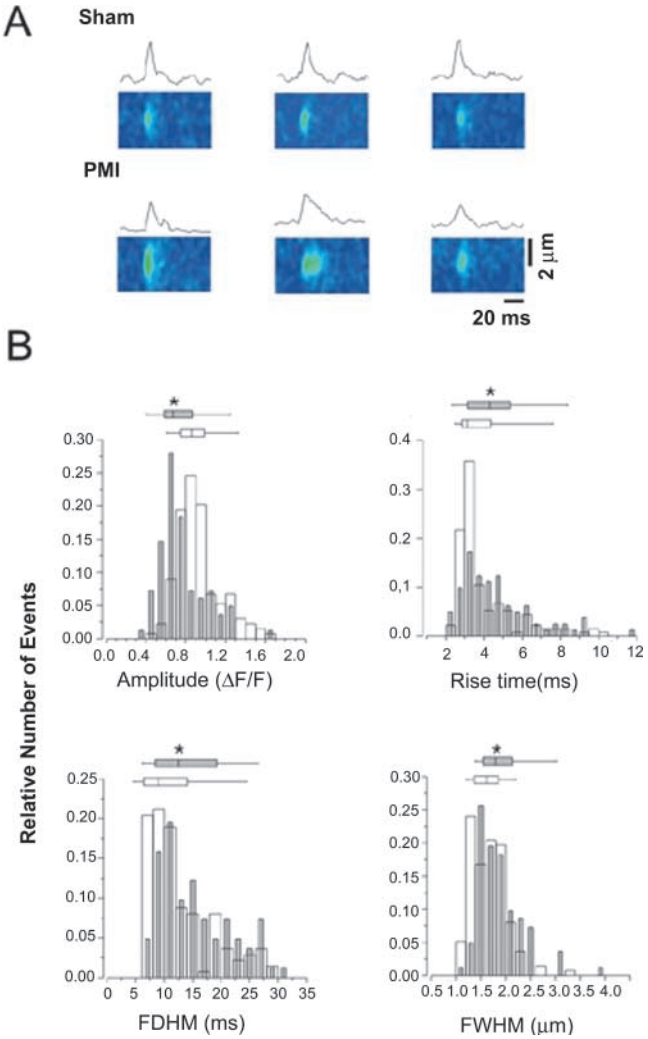

Figure 5. **Defects in local Ca^{2+} signaling in HF skeletal muscle.** (A) ΔF/F line scan images of representative examples of Ca^{2+} sparks in muscles from sham and postmyocardial infarction (PMI) HF rats and Ca^{2+} sparks time course. (B) Relative distributions of the spatio-temporal properties of Ca^{2+} sparks. Charts indicate 25, 50, 75 percentiles, the horizontal lines indicate the range from 1–99% of the distribution. Sham, open symbols ($n = 137$, three animals); postmyocardial infarction (PMI), gray symbols ($n = 82$, two animals). *, $P < 0.05$. FDHM, full duration at 1/2 peak amplitude; FWHM, full width at 1/2 peak amplitude.

FKBP12 (Brillantes et al., 1994; Marx et al., 1998) and of native RyR1 after removal of FKBP12 (Ahern et al., 1997; Marx et al., 1998). Similar defects in RyR1 single channel properties were observed in RyR1 isolated from skeletal muscle from FKBP12-null mice, although these animals die in utero or shortly after birth due to a developmental defect and skeletal muscle function could not be assessed (Shou et al., 1998).

Altered SR Ca^{2+} release in HF skeletal muscle

Ca^{2+} sparks, which represent SR Ca^{2+} release from clusters of individual RyR1, were examined in myotubes from sham-operated control and HF rat skeletal muscles (Fig. 5 A). SR Ca^{2+} release (sparks) amplitude was significantly reduced in skeletal myotubes from HF muscles with PKA-hyperphosphorylated RyR1, ΔF/F = 0.92 ± 0.02 (sham-operated control) versus 0.76 ± 0.03 in HF ($n = 6$; $P < 0.01$; Fig. 5 B). HF skeletal muscle Ca^{2+} sparks exhibited slower rise time

Table II. **Properties of RyR1 channels from normal and HF skeletal muscle**

	Channels active at resting $[Ca^{2+}]$	Channels with substates	Channels exhibiting coupled gating[a]	Open time	Closed time
				ms	*ms*
Normal skeletal muscle	0/53 (0%)	1/53 (2%)	6/53 (11%)	6.8 ± 1.3	9.7 ± 1.2
HF skeletal muscle	16/42 (38%)[b]	33/42 (78%)[c]	0/42 (0%)[c]	1.4 ± 0.3[c]	1.2 ± 0.2[c]

[a]We previously showed that in normal skeletal muscle, ~10% of RyR1 channels remain physically coupled to one another during isolation and insertion into the bilayer, so the level of coupled gating observed in the present study for RyR1 from control skeletal muscle is comparable to that in normal non-HF RyR1 (Marx et al., 1998).
[b]$P < 0.01$ for HF versus normal skeletal muscle.
[c]$P < 0.001$ for HF versus normal skeletal muscle.

(3.98 ± 0.14 [control] vs. 4.66 ± 0.21 ms [HF]; $P < 0.05$) and prolonged half duration (12.91 ± 0.50 [control] vs. 15.46 ± 0.69 ms [HF]; $P < 0.05$) (Fig. 5 B). Spatial spread of Ca^{2+} sparks was larger in the HF skeletal muscles (1.65 ± 0.03 vs. 1.95 ± 0.09 μm; $P < 0.05$; Fig. 5 B). Thus, PKA-hyperphosphorylated RyR1 is associated with slowed, reduced amplitude, longer-lasting SR Ca^{2+} release events.

RyR1 PKA phosphorylation correlates with defective muscle function in HF skeletal muscle

We next sought to determine whether PKA hyperphosphorylation of RyR1 and depletion of FKBP12 from the RyR1 complex are associated with impaired skeletal muscle function in a rodent postmyocardial infarction HF model. In this model, HF develops over 6 mo after myocardial infarction after ligation of the left anterior descending coronary artery. HF was documented with echocardiography, showing that fractional shortening was reduced to 41.4 ± 4.7% in HF ($n = 10$) versus 51.6 ± 5.3% in sham-operated control ($n = 6$; $P < 0.01$); fractional area of contraction was reduced in HF, 39.1 ± 5.1% versus 68.7 ± 2.4% in control ($P < 0.01$; HF vs. sham-operated control). Hemodynamics confirmed HF (LV end diastolic pressure = 9.16 ± 5.19 mm Hg for sham-operated control [$n = 6$] vs. 18.28 ± 8.56 mm Hg for HF [$n = 10$], $P < 0.05$; dP/dt = 5483 ± 1704 mm Hg/s for control vs. 2922 ± 784 mm Hg/s for HF, $P < 0.01$).

RyR1 was PKA hyperphosphorylated in rat HF skeletal muscle ($n = 10$) compared with sham-operated controls (Fig. 6 A; $n = 6$, $P < 0.01$), and the amount of FKBP12 bound to RyR1 was depleted by 58% in the HF skeletal muscle (Fig. 6 B; $P < 0.01$), although the total cellular levels of FKBP12 were not decreased in HF skeletal muscle (Fig. 6 C). Moreover, in contrast to the cardiac muscle RyR2 macromolecular complex in which PP1 and PP2A levels were decreased in HF, providing a potential explanation for the PKA hyperphosphorylation of the RyR2 channel (Marx et al., 2000), the amount of PP1 in the RyR1 complex was not decreased in HF skeletal muscle (Fig. 6 B). Recent studies have reported that the phosphodiesterase PDE4D3 and the targeting protein muscle A-kinase anchoring protein (mAKAP) form a signaling complex along with PKA (Dodge et al., 2001). Because we had previously shown that PKA is part of the RyR1 macromolecular complex (Marx et al., 2001) and PKA and mAKAP are components of the RyR2 complex (Marx et al., 2000), we sought to determine whether mAKAP and PDE4D3 were present in the RyR1 macromolecular complex. Indeed, using immunoprecipitation with anti–RyR-5029 and immunoblotting with antibodies that detect mAKAP and PDE4D3 (Fig. 6 D), we found that both mAKAP and PDE4D3 coimmunoprecipitate with RyR1 and therefore are likely part of the RyR1 macromolecular complex (Fig. 6 B). Moreover, compared with controls ($n = 4$), the amount of PDE4D3 in the RyR1 complex was significantly reduced in HF skeletal muscle ($n = 4$; $P < 0.05$; Fig. 6 B). The decreased PDE4D3 levels in the RyR1 channel complex could contribute to a local increase in cAMP and increased PKA activity, which may explain PKA hyperphosphorylation of RyR1 in HF skeletal muscle (Fig. 3 A; Fig. 6 A).

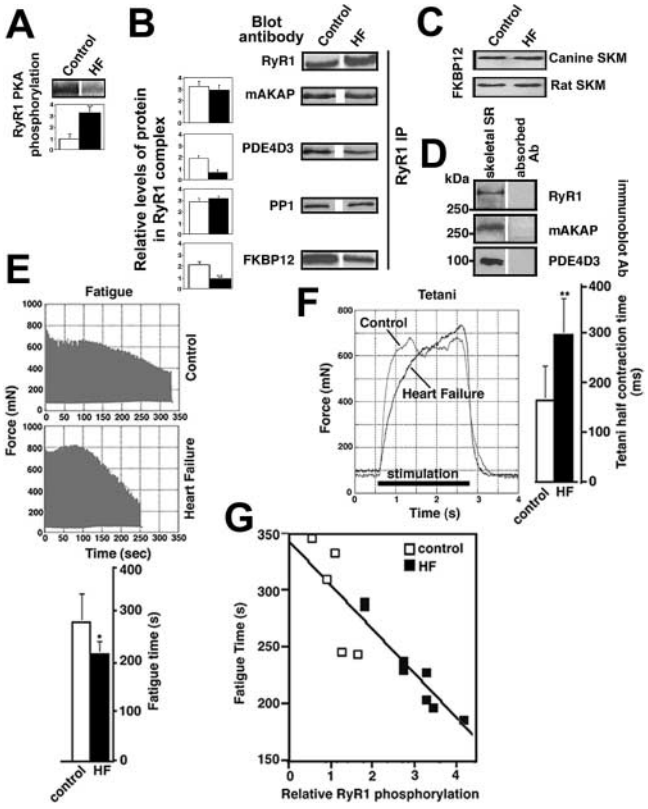

Figure 6. **RyR1 PKA phosphorylation and muscle fatigue.** (A) Autoradiogram showing PKA back phosphorylation of RyR1 from skeletal muscle of sham-operated (control) and HF rats, bar graph shows relative PKA phosphorylation of RyR1 (expressed as inverse of back phosphorylation as previously described [Marx et al., 2000]). (B) Immunoblots and bar graphs showing relative amounts of RyR1, mAKAP, PDE4D3, PP1, and FKBP12 immunoprecipitated with anti-RyR1 antibody from control and HF skeletal muscle. (C) Immunoblots showing equal amounts of total cellular FKBP12 in control and HF canine and rat skeletal muscles. (D) Immunoblots showing RyR1, mAKAP, and PDE4D3 detected in 100 μg human skeletal muscle SR; negative controls are with antibodies preabsorbed with the corresponding antigenic peptides. (E) HF skeletal muscle fatigues earlier than control. Rat soleus muscle ($n = 5$ control, $n = 8$ HF) was mounted in a tissue bath to assess contractile function (see Materials and methods for muscle function protocols). Representative fatigue time tracing is shown for control and HF skeletal muscles. Bar graph shows mean (±SD) time to fatigue. *, $P < 0.05$. (F) HF skeletal muscle achieved tetani more slowly than control. Tetani was induced by high-frequency stimulation as described in the Materials and methods. Bar graph shows tetani 1/2 contraction time. **, $P < 0.01$. (G) Correlation between time to fatigue and RyR1 PKA phosphorylation ($r = 0.88$) in rat skeletal muscle from sham and HF animals. Muscle function and RyR1 PKA phosphorylation were assessed using contralateral soleus muscles from each animal.

HF soleus muscles fatigued earlier and reached tetani more slowly than muscle from sham controls (Fig. 6, E and F). The fatigue time was 280 ± 59 s for control soleus muscle compared with 216 ± 26 s for HF soleus muscle ($n = 5$ sham-operated control, $n = 8$ HF; $P < 0.05$; Fig. 6 E). The tetanus half contraction time was 164.6 ± 70.1 ms for control soleus muscle compared with 297.5 ± 74.1 ms for HF soleus muscle ($n = 5$ sham control, $n = 8$ HF; $P < 0.01$; Fig. 6 F). The demonstration of defective contractile function, including delayed tetani and accelerated fatigue in HF

skeletal muscle, agrees with the findings of others (Perreault et al., 1993; Lunde et al., 2002). Moreover, the degree of RyR1 PKA hyperphosphorylation correlated significantly with early skeletal muscle fatigue ($r = 0.88$; Fig. 6 G). Thus, PKA hyperphosphorylation of RyR1 and depletion of FKBP12 from the RyR1 macromolecular complex are associated with altered skeletal muscle function.

Discussion

RyRs are involved in signaling in many types of cells, but the physiologic mechanisms that modulate the function of these intracellular Ca^{2+} release channels are not well understood. One of the best understood systems that involves RyRs is EC coupling in striated muscles, where RyRs are required for SR Ca^{2+} release, which activates muscle contraction. However, even in skeletal and cardiac muscles, the mechanisms by which systemic signals, such as the sympathetic nervous system (SNS), modulate RyR function remain to be elucidated.

The "fight or flight" response is a classic stress pathway that involves activation of the SNS, leading to β-adrenergic stimulation of muscle. During SNS stimulation, catecholamines bind to β-adrenergic receptors, activate adenylyl cyclase via G-proteins, and increase the intracellular levels of the second messenger cAMP, which activates PKA. In the present study, we have shown that PKA phosphorylation activates RyR1 channels by phosphorylating them on Ser^{2843}. This PKA phosphorylation site that we identified using site-directed mutagenesis agrees with previous studies in which the same site was identified by phosphopeptide mapping (Suko et al., 1993). Identification of the PKA phosphorylation site on RyR1 Ser^{2843} allowed us to generate the mutant RyR1 required to probe the mechanism by which PKA phosphorylation activates RyR1 channels. This approach allowed us to determine that PKA phosphorylation activates RyR1 by phosphorylating Ser^{2843}, which causes dissociation of FKBP12 from the channel. The dissociation of FKBP12 relieves an inhibition of channel opening that is due to the stabilization of RyR1 channels in the closed state when FKBP12 is bound.

Data from the present study provide novel insights regarding the mechanism by which FKBP12 modulates RyR1 function in the context of skeletal muscle EC coupling. The original studies on the role of FKBP12 in the RyR1 channel complex suggested that this 12-kD protein was involved in stabilizing RyR1 channels, possibly via binding to the channel and stabilizing it in a favorable conformation that is required for normal physiologic function during EC coupling (Jayaraman et al., 1992; Brillantes et al., 1994). We now show that PKA phosphorylation of RyR1 activates the channel by dissociating FKBP12 from the channel complex. This finding suggests that one physiologic role of FKBP12 is to stabilize the closed state of the channel, essentially acting as a natural channel inhibitor. By releasing FKBP12 from the channel complex, PKA phosphorylation relieves this inhibition and activates the channel. PKA phosphorylation of RyR1 provides a physiologic mechanism for increasing RyR1 activity. Even though our data indicate that FKBP12 stabilizes RyR1 open and closed states, because RyR1 channels are opened via an interaction with the VGCC in skeletal muscle (Schneider and Chandler, 1973; Rios and Brum, 1987), the more important role for FKBP12 in the RyR1 macromolecular complex in skeletal muscle likely is to stabilize the closed state of the channel (i.e., FKBP12 may help keep RyR1 channels closed when muscle is relaxed and prevent SR Ca^{2+} leak in skeletal muscle).

To determine the physiologic consequence of our finding that PKA phosphorylation activates RyR1, which is in agreement with previous reports (Hain et al., 1994; Sonnleitner et al., 1997), we chose to compare the function of normal skeletal muscle with those from animal models of HF. HF is a hyperadrenergic state (Chidsey et al., 1962), and our data showing that RyR1 is PKA hyperphosphorylated in HF skeletal muscle provided us with a model in which we would compare the function of muscles with and without PKA-phosphorylated RyR1 in order to probe the role of this form of regulation of RyR1 in skeletal muscle function.

In skeletal muscle, Ca^{2+} sparks representing elementary Ca^{2+} release events arising from a cluster of RyR1 channels (Gonzalez et al., 2000) have been technically difficult to record from adult mammalian skeletal muscle (Shirokova et al., 1998; Kirsch et al., 2001). In HF skeletal muscle, Ca^{2+} sparks exhibited reduced amplitude, slowed rise time, and prolonged duration. Depletion of FKBP12 from RyR1 might cause an SR Ca^{2+} leak, which could deplete SR Ca^{2+} and contribute to reduced amplitude of SR Ca^{2+} release events observed in HF skeletal muscle. The muscle fibers were saponin skinned, and free $[Ca^{2+}]$ was clamped at 130 nM. These conditions likely explain why the spark frequency was not significantly increased in HF skeletal muscle, because the overall spark frequency was very low at resting $[Ca^{2+}]$ of 130 nM. Clamping the free Ca^{2+} at 130 nM could also explain why there was not a significant decrease in SR Ca^{2+} content in HF skeletal muscle, measured using acute application of 4-chloro-m-cresol (caffeine analogue), because SR Ca^{2+} ATPase activity combined with the low spark rate, in part due to clamping free Ca^{2+} at a low (resting) level, would favor refilling the SR. We have described coupled gating between RyR1 channels as a mechanism that enables groups of channels that are physically contacting one another in the SR membrane to open and close as a single Ca^{2+} release unit (Marx et al., 1998). FKBP12 binding to RyR1 is required for coupled gating (Marx et al., 1998). Reduced coupled gating due to FKBP12 depletion could slow the rate of SR Ca^{2+} release and impair RyR1 channel closure, contributing to the prolonged decay of the SR Ca^{2+} release transient.

HF skeletal muscles containing PKA-hyperphosphorylated RyR1 exhibited prolonged tetani half-contraction times. Prolonged tetani half-time (meaning that it takes longer to achieve tetani with the same repetitive stimuli) could reflect impaired EC coupling, which may occur due to FKBP12 depletion (Lamb and Stephenson, 1996), although the specific role of FKBP12 in normal skeletal muscle EC coupling remains to be elucidated. The early fatigue in HF skeletal muscle correlates strongly with increased PKA phosphorylation of RyR1, suggesting a functional association between these two findings. Because there is very little Ca^{2+} entry or extrusion in skeletal myocytes, they must recycle

most of the Ca^{2+} required for EC coupling. One cost of compensating for increased SR Ca^{2+} leakage due to PKA-hyperphosphorylated RyR1 channels that are depleted of FKBP12 in skeletal muscle may be increased energy consumption (ATP is required to pump Ca^{2+} back into the SR via the Ca^{2+}-ATPase), which could contribute to the early fatigue observed in HF skeletal muscle.

The significance of a primary skeletal muscle defect in HF is underscored by the fact that fatigue in patients does not correlate well with cardiac function (Harrington and Coats, 1997). The problem with skeletal muscle does not appear to be simply a matter of impaired skeletal muscle blood flow, as administration of angiotensin-converting enzyme inhibitors (Drexler et al., 1989) or cardiac transplantation (Stratton et al., 1994; Sorensen et al., 1999) both increase cardiac output and skeletal muscle blood flow but do not improve skeletal muscle function. Studies have documented alterations in skeletal muscle energy metabolism in HF, including increased lactate production and turnover (Katz et al., 1993; Wilson et al., 1993), more rapid breakdown of phosphocreatine, and reduced phosphocreatine resynthesis (Mancini et al., 1992).

Defects in SR Ca^{2+} release channel function and Ca^{2+} signaling provide a mechanism that could underlie the impaired skeletal muscle function in HF. The underlying pathology driving the EC coupling myopathy in cardiac and skeletal muscles is probably the chronic hyperadrenergic state that leads to defective SR Ca^{2+} release channel function through PKA hyperphosphorylation of both RyR1 and RyR2. Support for the adverse role of the chronic hyperadrenergic state in HF comes from recent studies showing that β-adrenergic receptor blockers improve cardiac function in HF, reverse PKA hyperphosphorylation of RyR2, and normalize channel function (Reiken et al., 2001; Doi et al., 2002). However, β blockers have only modest benefit, or none at all, in terms of improved exercise tolerance in patients with HF (Kukin et al., 1999; Gullestad et al., 2001). β blockers have complex effects on skeletal muscle energy metabolism, for example, propranolol inhibits β-adrenergic–induced activation of both phosphorylase kinase and glycogen synthase (Dietz et al., 1980). Thus, it is possible that beneficial effects of β blockade, in terms of improved skeletal muscle function, could be balanced by adverse effects on energy metabolism, resulting in only minimal improvement in exercise tolerance.

Combined with our previous studies (Marx et al., 2000), the present data indicate that HF may be characterized as a generalized EC coupling myopathy that affects both forms of striated muscles, cardiac and skeletal. The underlying pathology that causes this general EC coupling myopathy is likely the chronic hyperadrenergic state that occurs during HF. The implications of these new understandings include the possibility that novel therapeutic targets for HF exist in the components of the RyR1 and RyR2 macromolecular complexes that regulate PKA phosphorylation and dephosphorylation of the channels.

Materials and methods

Recombinant RyR1

Recombinant WT and mutant RyR1 were expressed, isolated, and characterized as previously described (Brillantes et al., 1994; Gaburjakova et al., 2001). 48 h after transfection, cells were washed two times, scraped into PBS, and pelleted by centrifugation at 2,500 *g* for 5 min at 4°C. Microsomes were prepared, aliquoted, and stored at −80°C as previously described (Gaburjakova et al., 2001).

Immunoblots, immunoprecipitations, and phosphorylation

Skeletal muscle lysates were prepared from 1.0 g of canine tissue or whole rat soleus muscles homogenized in 1.0 ml of buffer, 50 mM Tris-HCl (pH 7.4), 200 mM NaCl, 20 mM NaF, 1.0 mM Na_3VO_4, 1.0 mM DTT, and protease inhibitors. Samples were centrifuged at 3,000 *g* for 10 min and supernatants stored at −80°C. For immunoprecipitations, skeletal SR samples were resuspended in 0.5 ml of IP buffer (50 mM Tris-HCl [pH 7.4], 0.9% NaCl, 0.5 mM NaF, 0.5 mM Na_3VO_4, 0.25% Triton X-100, and protease inhibitors) and incubated with anti-RyR antibody overnight at 4°C. Immunoblots were performed using the following primary antibodies: anti–PKA catalytic subunit (1:1,000), anti-PP1 (1:1,000; Transduction Labs), anti-FKBP (1:1,000; Jayaraman et al., 1992), anti–RyR-5029 (1:3,000; Jayaraman et al., 1992), anti-PDE4D3 (1:1,000; affinity-purified polyclonal antibody raised in rabbits immunized with a mixture of two PDE4D3 peptides, residues 1–14 of human PDE4D3 with a carboxy-terminal cysteine added for conjugation to keyhole limpet hemocyanin, and the corresponding rat sequence that has a T instead of an N at residue 6, MMHVNN/TFP-FRRHSW[C]), anti-mAKAP (1:750; affinity purified polyclonal antibody raised in rabbits immunized with a peptide corresponding to mAKAP sequence with an amino-terminal cysteine added for conjugation to keyhole limpet hemocyanin, [C]ETRFNNRQDSDALKSSDD). Protein A–sepharose beads were added, incubated at 4°C for 1 h, and washed three times with IP buffer. For phosphorylations, beads were washed with 1X phosphorylation buffer (8 mM MgCl, 10 mM EGTA, 50 mM Tris/piperazine-N,N′-bis[2-ethanesulfonic acid], pH 6.8) and resuspended in 10 μl of 1.5X phosphorylation buffer containing vehicle alone, PKA catalytic subunit (5 U; Sigma-Aldrich), PKA plus PKA inhibitor (PKI_{5-24}; 500 nM; Calbiochem), or cAMP (10 μM). Phosphorylation of immunoprecipitated RyR1 was initiated with MgATP (33 μM), [γ^{32}P]-ATP, and terminated after incubation for 5 min at RT with 5 μl stop solution (4% SDS and 0.25 M DTT). For dephosphorylation experiments, the cAMP reaction was terminated by addition of PKI, followed by addition of protamine (1 mg/ml) ± okadaic acid (5 μM). Samples were heated to 95°C and size fractionated on 6% SDS-PAGE, and RyR2 radioactivity was quantified using a Molecular Dynamics Phosphorimager and ImageQuant software (Amersham Biosciences). Nonspecific phosphorylation (not inhibited by PKI) was subtracted, and the ^{32}P/RyR1 ratio was calculated by dividing ^{32}P phosphorylation by the amount of high-affinity [^{3}H]ryanodine binding (one high-affinity ryanodine binding site per RyR1). All experiments were performed in triplicate, and the investigator was blinded to the source of samples.

FKBP12 binding

Microsomes (200 μg) were resuspended in 0.1 ml imidazole buffer (5 mM imidazole, pH 7.4, and 0.3 M sucrose), containing protease inhibitors, and incubated with Mg-ATP (100 μM) and either PKA (10 U) or cAMP (10 μM) at 30°C for 30 min. Samples were centrifuged at 95,000 *g* for 10 min, and supernatants were collected. Pellets were washed twice in 0.2 ml imidazole buffer and centrifuged at 95,000 *g* for 10 min. The final pellet was resuspended in 0.1 ml imidazole buffer. In some experiments, pellets were phosphorylated with cAMP and then dephosphorylated with alkaline phosphatase (1:100 enzyme/protein) or by activating endogenous phosphatases with protamine (1 mg/ml). Recombinant FKBP12 was added to these samples for 4 h at 4°C to allow binding to RyR1. Pellet and supernatant were size fractionated by SDS-PAGE and immunoblotted for FKBP12.

Single channel recordings

SR vesicles from control or HF skeletal muscle, or vesicles from HEK 293 cells transfected with recombinant WT or mutant RyR1 were incorporated into planar lipid bilayers, and single channel recordings of RyR1 were performed as previously described (Brillantes et al., 1994; Gaburjakova et al., 2001). Microsomes containing WT RyR1 were phosphorylated with PKA as described above. Solutions used for channel analysis were as follows: trans solution (250 mM Hepes, 53 mM $Ca[OH]_2$, 50 mM KCl, pH 7.35) and cis solution (250 mM Hepes, 125 mM Tris, 50 mM KCl, 1 mM EGTA, 0.5 mM $CaCl_2$, pH 7.35). Free [Ca^{2+}] in the cis compartment was calculated using the Chelator software (Schoenmakers et al., 1992). Single channel currents were filtered at 1 kHz and digitized at 4 kHz. pClamp 6 (Axon Instruments, Inc.) was used for analyzing single channel data. Open probability, the lifetime of open events, and gating frequency were identified by 50% threshold analysis using ≥2 min of continuous record. At the conclusion of each experiment, ryanodine (5 μM) was applied to the cis chamber to confirm channels as RyRs. Mean open and closed dwell time analysis

was performed using Fetchan software (Axon Instruments, Inc.), and open time distribution was fitted with a two-exponential least-square regression analysis as previously described (Marx et al., 2001). Data are mean ± SEM. The unpaired *t* test was used for statistical comparison of mean values; $P < 0.05$ was considered significant.

Animal models of HF

Rapid LV pacing induced HF as previously described (Wang et al., 1997). Nine dogs (28–30 kg) were used: (a) normal without heart instrumentation ($n = 4$) and (b) HF ($n = 5$). After baseline measurements, rapid LV pacing was initiated at 210 bpm for 3 wks, followed by 1 wk pacing at 240 bpm with an external pacemaker (EV4543; Pace Medical, Inc.). 12 Sprague-Dawley (300–400 g) and 2 Wistar rats underwent left coronary ligation via left thoracotomy, and 6 Sprague-Dawley and 3 Wistar rats underwent sham operations (control). After 1 wk, echocardiography was performed on all rats. 6 mo after coronary ligation, echocardiography was repeated, and hemodynamic data were collected. Animals were then killed and soleus muscles harvested.

Ca^{2+} sparks

Bundles of 4–7 fibers were manually dissected from extensor digitorus longum muscle in a relaxing solution (in mM: K-glutamate 140, Hepes 10, $MgCl_2$ 10, EGTA 0.1, pH 7.0), mounted as previously described (Lacampagne et al., 1998), and permeabilized in the relaxing solution containing 0.01% saponin for 30–40 s. The solution was changed to an internal medium (in mM: K-glutamate 140, Na_2ATP 5, glucose 10, Hepes 10, $MgCl_2$ 4.4, EGTA 1.1, $CaCl_2$ 0.3, Fluo-3 0.05 [pentapotassium salt; Tef-labs], pH 7.0) used for image recording. Fluorescence images were acquired with a Carl Zeiss MicroImaging, Inc. LSM 510 NLO confocal system (63x oil immersion, NA 1.4) operated in line-scan mode (x vs. t, 1.9 ms/line). Fluo-3 was excited with an argon/kryton laser at 488 nm, and emitted fluorescence was recorded at ~525 nm. Potential spark areas were empirically identified using an autodetection algorithm (Cheng et al., 1999). The mean F value for the image was calculated by summing and averaging the temporal F at each spatial location while ignoring potential spark areas. This F value was then used to create a $\Delta F/F$ image pixel by pixel. Selection and analysis of Ca^{2+} sparks were performed essentially as previously described (Klein et al., 1997). Determinations of spatio-temporal properties of individual Ca^{2+} sparks were made on spatial (x) and temporal (t) profiles of sparks centered at the peak amplitude. The $\Delta F/F$ amplitude as well as temporal parameters, rise time (10–90% of peak $\Delta F/F$, RT), and duration (full duration at half-maximum peak amplitude, FDHM) were derived from the temporal profile. The width of the Ca^{2+} spark (full width at half-maximum peak amplitude, FWHM) was determined from the spatial profile. Statistical comparison of population parameters between the two groups was conducted using a nonparametric Kruskal-Wallis test.

Muscle function

Soleus muscles were attached to a force transducer in a water bath (Harvard Apparatus) and perfused with Krebs-Henseleit containing 2 mM Ca^{2+} bubbled with 5% CO_2/95% O_2. The muscle was rested for 60 min and then stimulated with single pulses at 10-s intervals. The twitch force, twitch contraction time, and half-relaxation time were measured. Stimulation was at 1 Hz at 1–30 V. The tetani force, half-contraction time, and half-relaxation time were also determined by using a stimulating frequency and titanic duration of 50 Hz and 600 ms (Lunde et al., 2001). Fatigue was produced by inducing a tetanus every 2 s and measuring the time for force to fall to 40% of the maximum.

This work was supported by grants to A.R. Marks from the National Institutes of Health, the American Heart Association, and the Whitaker Foundation (S. Reiken). A.R. Marks is a Doris Duke Charitable Foundation Distinguished Clinical Scientist.

Submitted: 4 November 2002
Revised: 3 February 2003
Accepted: 3 February 2003

References

Ahern, G.P., P.R. Junankar, and A.F. Dulhunty. 1997. Subconductance states in single-channel activity of skeletal muscle ryanodine receptors after removal of FKBP12. *Biophys. J.* 72:146–162.

Brillantes, A.B., K. Ondrias, A. Scott, E. Kobrinsky, E. Ondriasova, M.C. Moschella, T. Jayaraman, M. Landers, B.E. Ehrlich, and A.R. Marks. 1994. Stabilization of calcium release channel (ryanodine receptor) function by FK506-binding protein. *Cell.* 77:513–523.

Cheng, H., L.S. Song, N. Shirokova, A. Gonzalez, E.G. Lakatta, E. Rios, and M.D. Stern. 1999. Amplitude distribution of calcium sparks in confocal images: theory and studies with an automatic detection method. *Biophys. J.* 76: 606–617.

Chidsey, C.A., D.C. Harrison, and E. Braunwald. 1962. Augmentation of plasma norepinephrine response to exercise in patients with congestive heart failure. *N. Engl. J. Med.* 267:650–658.

Dietz, M.R., J.L. Chiasson, T.R. Soderling, and J.H. Exton. 1980. Epinephrine regulation of skeletal muscle glycogen metabolism. Studies utilizing the perfused rat hindlimb preparation. *J. Biol. Chem.* 255:2301–2307.

Dodge, K.L., S. Khouangsathiene, M.S. Kapiloff, R. Mouton, E.V. Hill, M.D. Houslay, L.K. Langeberg, and J.D. Scott. 2001. mAKAP assembles a protein kinase A/PDE4 phosphodiesterase cAMP signaling module. *EMBO J.* 10: 1921–1930.

Doi, M., M. Yano, S. Kobayashi, M. Kohno, T. Tokuhisa, S. Okuda, M. Suetsugu, Y. Hisamatsu, T. Ohkusa, and M. Matsuzaki. 2002. Propranolol prevents the development of heart failure by restoring FKBP12.6-mediated stabilization of ryanodine receptor. *Circulation.* 105:1374–1379.

Drexler, H., U. Banhardt, T. Meinertz, H. Wollschlager, M. Lehmann, and H. Just. 1989. Contrasting peripheral short-term and long-term effects of converting enzyme inhibition in patients with congestive heart failure. A double-blind, placebo-controlled trial. *Circulation.* 79:491–502.

Fabiato, A. 1983. Calcium-induced release of calcium from the cardiac sarcoplasmic reticulum. *Am. J. Physiol.* 245:C1–C14.

Gaburjakova, M., J. Gaburjakova, S. Reiken, F. Huang, S.O. Marx, N. Rosemblit, and A.R. Marks. 2001. FKBP12 binding modulates ryanodine receptor channel gating. *J. Biol. Chem.* 276:16931–16935.

Gonzalez, A., W.G. Kirsch, N. Shirokova, G. Pizarro, G. Brum, I.N. Pessah, M.D. Stern, H. Cheng, and E. Rios. 2000. Involvement of multiple intracellular release channels in calcium sparks of skeletal muscle. *Proc. Natl. Acad. Sci. USA.* 97:4380–4385.

Gullestad, L., C. Manhenke, T. Aarsland, R. Skardal, H. Fagertun, J. Wikstrand, and J. Kjekshus. 2001. Effect of metoprolol CR/XL on exercise tolerance in chronic heart failure-a substudy to the MERIT-HF trial. *Eur. J. Heart Fail.* 3:463–468.

Hain, J., S. Nath, M. Mayrleitner, S. Fleischer, and H. Schindler. 1994. Phosphorylation modulates the function of the calcium release channel of sarcoplasmic reticulum from skeletal muscle. *Biophys. J.* 67:1823–1833.

Hain, J., H. Onoue, M. Mayrleitner, S. Fleischer, and H. Schindler. 1995. Phosphorylation modulates the function of the calcium release channel of sarcoplasmic reticulum from cardiac muscle. *J. Biol. Chem.* 270:2074–2081.

Harrington, D., and A.J. Coats. 1997. Mechanisms of exercise intolerance in congestive heart failure. *Curr. Opin. Cardiol.* 12:224–232.

Jayaraman, T., A.-M.B. Brillantes, A.P. Timerman, H. Erdjument-Bromage, S. Fleischer, P. Tempst, and A.R. Marks. 1992. FK506 binding protein associated with the calcium release channel (ryanodine receptor). *J. Biol. Chem.* 267:9474–9477.

Kaftan, E., A.R. Marks, and B.E. Ehrlich. 1996. Effects of rapamycin on ryanodine receptor/$Ca^{(2+)}$-release channels from cardiac muscle. *Circ. Res.* 78:990–997.

Katz, S.D., B. Bleiberg, J. Wexler, K. Bhargava, J.J. Steinberg, and T.H. LeJemtel. 1993. Lactate turnover at rest and during submaximal exercise in patients with heart failure. *J. Appl. Physiol.* 75:1974–1979.

Kirsch, W.G., D. Uttenweiler, and R.H. Fink. 2001. Spark- and ember-like elementary Ca^{2+} release events in skinned fibres of adult mammalian skeletal muscle. *J. Physiol.* 537:379–389.

Klein, M.G., A. Lacampagne, and M.F. Schneider. 1997. Voltage dependence of the pattern and frequency of discrete Ca^{2+} release events after brief reprimming in frog skeletal muscle. *Proc. Natl. Acad. Sci. USA.* 94:11061–11066.

Kukin, M.L., J. Kalman, R.H. Charney, D.K. Levy, C. Buchholz-Varley, O.N. Ocampo, and C. Eng. 1999. Prospective, randomized comparison of effect of long-term treatment with metoprolol or carvedilol on symptoms, exercise, ejection fraction, and oxidative stress in heart failure. *Circulation.* 99:2645–2651.

Lacampagne, A., M.G. Klein, and M.F. Schneider. 1998. Modulation of the frequency of spontaneous sarcoplasmic reticulum Ca^{2+} release events (Ca^{2+} sparks) by myoplasmic [Mg^{2+}] in frog skeletal muscle. *J. Gen. Physiol.* 111: 207–224.

Lamb, G.D., and D.G. Stephenson. 1996. Effects of FK506 and rapamycin on excitation-contraction coupling in skeletal muscle fibres of the rat. *J. Physiol.* 494:569–576.

Lunde, P.K., A.J. Dahlstedt, J.D. Bruton, J. Lannergren, P. Thoren, O.M. Sejer-

sted, and H. Westerblad. 2001. Contraction and intracellular Ca^{2+} handling in isolated skeletal muscle of rats with congestive heart failure. *Circ. Res.* 88: 1299–1305.

Lunde, P.K., E. Verburg, M. Eriksen, and O.M. Sejersted. 2002. Contractile properties of in situ perfused skeletal muscles from rats with congestive heart failure. *J. Physiol.* 540:571–580.

Mancini, D.M., G. Walter, N. Reichek, R. Lenkinski, K.K. McCully, J.L. Mullen, and J.R. Wilson. 1992. Contribution of skeletal muscle atrophy to exercise intolerance and altered muscle metabolism in heart failure. *Circulation.* 85: 1364–1373.

Marks, A.R. 1996. Cellular functions of immunophilins. *Physiol. Rev.* 76:631–649.

Marx, S.O., K. Ondrias, and A.R. Marks. 1998. Coupled gating between individual skeletal muscle Ca^{2+} release channels (ryanodine receptors). *Science.* 281: 818–821.

Marx, S.O., S. Reiken, Y. Hisamatsu, T. Jayaraman, D. Burkhoff, N. Rosemblit, and A.R. Marks. 2000. PKA phosphorylation dissociates FKBP12.6 from the calcium release channel (ryanodine receptor): defective regulation in failing hearts. *Cell.* 101:365–376.

Marx, S.O., S. Reiken, Y. Hisamatsu, M. Gaburjakova, J. Gaburjakova, Y.M. Yang, N. Rosemblit, and A.R. Marks. 2001. Phosphorylation-dependent regulation of ryanodine receptors. A novel role for leucine/isoleucine zippers. *J. Cell Biol.* 153:699–708.

Meissner, G. 1994. Ryanodine receptor/Ca^{2+} release channels and their regulation by endogenous effectors. *Annu. Rev. Physiol.* 56:485–508.

Minotti, J.R., I. Christoph, R. Oka, M.W. Weiner, L. Wells, and B.M. Massie. 1991. Impaired skeletal muscle function in patients with congestive heart failure. Relationship to systemic exercise performance. *J. Clin. Invest.* 88: 2077–2082.

Nabauer, M., G. Callewaert, L. Cleemann, and M. Morad. 1989. Regulation of calcium release is gated by calcium current, not gating charge, in cardiac myocytes. *Science.* 244:800–803.

Perreault, C.L., H. Gonzalez-Serratos, S.E. Litwin, X. Sun, C. Franzini-Armstrong, and J.P. Morgan. 1993. Alterations in contractility and intracellular Ca^{2+} transients in isolated bundles of skeletal muscle fibers from rats with chronic heart failure. *Circ. Res.* 73:405–412.

Reiken, S., M. Gaburjakova, J. Gaburjakova, K.L. He, A. Prieto, E. Becker, G.H. Yi, J. Wang, D. Burkhoff, and A.R. Marks. 2001. β-Adrenergic receptor blockers restore cardiac calcium release channel (ryanodine receptor) structure and function in heart failure. *Circulation.* 104:2843–2848.

Rios, E., and G. Brum. 1987. Involvement of dihydropyridine receptors in excitation-contraction coupling in skeletal muscle. *Nature.* 325:717–720.

Schneider, M.F., and W.K. Chandler. 1973. Voltage-dependent charge movement in skeletal muscle: a possible step in excitation-contraction coupling. *Nature.* 242:244–246.

Schoenmakers, T.J., G.J. Visser, G. Flik, and A.P. Theuvenet. 1992. CHELATOR: an improved method for computing metal ion concentrations in physiological solutions. *Biotechniques.* 12:870–874.

Seiler, S., A.D. Wegener, D.D. Whang, D.R. Hathaway, and L.R. Jones. 1984. High molecular weight proteins in cardiac and skeletal muscle junctional sarcoplasmic reticulum vesicles bind calmodulin, are phosphorylated, and are degraded by Ca^{2+}-activated protease. *J. Biol. Chem.* 259:8550–8557.

Shirokova, N., J. Garcia, and E. Rios. 1998. Local calcium release in mammalian skeletal muscle. *J. Physiol.* 512:377–384.

Shou, W., B. Aghdasi, D.L. Armstrong, Q. Guo, S. Bao, M.J. Charng, L.M. Mathews, M.D. Schneider, S.L. Hamilton, and M.M. Matzuk. 1998. Cardiac defects and altered ryanodine receptor function in mice lacking FKBP12. *Nature.* 391:489–492.

Sonnleitner, A., S. Fleischer, and H. Schindler. 1997. Gating of the skeletal calcium release channel by ATP is inhibited by protein phosphatase 1 but not by Mg^{2+}. *Cell Calcium.* 21:283–290.

Sorensen, V.B., H. Wroblewski, S. Galatius, S. Haunso, and J. Kastrup. 1999. Exercise blood flow and microvascualr distensibility in skeletal muscle normalize after heart transplantation. *Clin. Transplant.* 13:410–419.

Stern, M.D., G. Pizarro, and E. Rios. 1997. Local control model of excitation-contraction coupling in skeletal muscle. *J. Gen. Physiol.* 110:415–440.

Stratton, J.R., G.J. Kemp, R.C. Daly, M. Yacoub, and B. Rajagopalan. 1994. Effects of cardiac transplantation on bioenergetic abnormalities of skeletal muscle in congestive heart failure. *Circulation.* 89:1624–1631.

Suko, J., I. Maurer-Fogy, B. Plank, O. Bertel, W. Wyskovsky, M. Hohenegger, and G. Hellmann. 1993. Phosphorylation of serine 2843 in ryanodine receptor-calcium release channel of skeletal muscle by cAMP-, cGMP- and CaM-dependent protein kinase. *Biochim. Biophys. Acta.* 1175:193–206.

Sullivan, M.J., and M.H. Hawthorne. 1995. Exercise intolerance in patients with chronic heart failure. *Prog. Cardiovasc. Dis.* 38:1–22.

Takasago, T., T. Imagawa, and M. Shigekawa. 1989. Phosphorylation of the cardiac ryanodine receptor by cAMP-dependent protein kinase. *J. Biochem. (Tokyo).* 106:872–877.

Uehara, A., M. Yasukochi, R. Mejia-Alvarez, M. Fill, and I. Imanaga. 2002. Gating kinetics and ligand sensitivity modified by phosphorylation of cardiac ryanodine receptors. *Pflugers Arch.* 444:202–212.

Valdivia, H.H., J.H. Kaplan, G.C. Ellis-Davies, and W.J. Lederer. 1995. Rapid adaptation of cardiac ryanodine receptors: modulation by Mg^{2+} and phosphorylation. *Science.* 267:1997–2000.

Wang, J., G.H. Yi, M. Knecht, B.L. Cai, S. Poposkis, M. Packer, and D. Burkhoff. 1997. Physical training alters the pathogenesis of pacing-induced heart failure through endothelium-mediated mechanisms in awake dogs. *Circulation.* 96:2683–2692.

Wilson, J.R., D.M. Mancini, and W.B. Dunkman. 1993. Exertional fatigue due to skeletal muscle dysfunction in patients with heart failure. *Circulation.* 87: 470–475.